

Colloidal Processing and Superplasticity of MgO and TiO₂-Added Y-ZrO₂ Fine-Grained Polycrystals

T. Matsumoto*, Y. Sakka**, T. S. Suzuki**, K. Morita**,
B. Kim**, K. Hiraga** and Y. Moriyoshi*

*:HOSEI UNIVERSITY, 3-7-2, Kajino-cho, Koganei, Japan

** : NATIONAL RESEARCH INSTITUTE FOR METALS, 1-2-1, Sengen, Tsukuba, Ibaraki, Japan

Fax: 81-0298-59-2461, e-mail ysakka@nrim.go.jp

The application of superplasticity to the manufacturing process is limited, because conventional superplastic ceramics require higher temperatures over 1400°C and a slower deformation rate of about 10⁻⁴ s⁻¹. The purpose of this study is to fabricate high-strain rate superplastic zirconias by adding MgO and TiO₂ to 3YTZ (3mol%Y₂O₃ doped ZrO₂). Dense and fine-grained zirconia polycrystals were obtained by colloidal processing, where aqueous suspensions were prepared by dispersing 3YTZ, MgO and TiO₂ powders by ultrasonication and adding the appropriate amount of polyelectrolyte. The grain growth was controlled by cation lattice diffusion and the grain growth rate was enhanced by adding TiO₂ and MgO. The tensile ductility of about 216% was established for the system of 3(Y₂O₃, MgO) · 97(Zr_{0.95}Ti_{0.05})O₂ at the low temperature of 1350°C and high strain rate of 1.2 × 10⁻² s⁻¹.

Key words: tetragonal zirconia, titania, grain growth, colloidal processing, superplasticity

1. INTRODUCTION

Superplasticity provides the possibility of the high-temperature deformation processing of dense ceramics and has the advantages of sharper formability with better dimensional accuracy. Superplastic ceramics have been widely studied ⁽¹⁾⁻⁽⁶⁾, since superplasticity was first reported in 1986 by Wakai et al. ⁽¹⁾. However, superplastic ceramics were only formed at relatively low-strain rates around 10⁻⁴ s⁻¹ and at higher temperatures above 1400°C. Recently, it was reported that the deformation rate was enhanced by adding TiO₂ to the ZrO₂ system ⁽²⁾. The objective of this study is to fabricate excellent superplastic ceramics by adding TiO₂ and MgO to 3Y-TZ (3mol% Y₂O₃ doped ZrO₂). Here, MgO was added to stabilize the tetragonal phase of the 3Y-TZ system. Preliminary studies have shown that certain requirements must be met to achieve superplasticity, i.e., fine-grain size, homogeneous microstructure and high density ⁽⁷⁾. In order to obtain a fine-grained size after sintering, fine particles must be used. However, fine particles tend to spontaneously agglomerate due to van der Waals forces. The agglomerated particles form large pores and a high temperature is necessary to eliminate the pores and form dense bodies. Colloidal processing helps to prevent the agglomeration of fine particles and allow the particle dispersion to be controlled during powder processing. Dispersed aqueous suspensions of 3YTZ, TiO₂ and MgO fine particles were prepared by adding an appropriate amount of polyelectrolyte with ultrasonication. The compacts, consolidated by slip casting,

have a narrow pore size distribution and are dense. Therefore, fine-grained and dense sintered specimens are obtained by low temperature sintering. The fine-grained 3YTZ ceramics with added TiO₂ and MgO shows high-strain rate superplasticity.

2. EXPERIMENTAL PROCEDURE

The raw powders of 3YTZ, TiO₂ and MgO used in this study were produced by Tosoh, Nanotek and Ube Industry, respectively. Average particles sizes of the 3YTZ, TiO₂ and MgO powders are 70, 30 and 50 nm, respectively. Long range segregation caused by the difference in the particle size and density during slip casting is prevented if the solid content of the suspension is more than 30vol%⁽⁹⁾. Therefore, aqueous suspensions containing 30vol% solids were prepared for the composition in the following chemical form, 3mol%(Y₂O₃,MgO) · 97(Zr_xTi_{1-x})O₂ ;(x=0.85, 0.90, 0.95). Hereafter, we express this composition as 3YM-xZT.

Re-dispersion is necessary to properly disperse a mixture of fine particles because of their agglomeration. The suspensions were ultrasonicated to homogeneously disperse 3YTZ, TiO₂ and MgO particles (20kHz, 160kW for 10min). Sufficient amount of polyelectrolyte (ammonium polyacrylate; Toa gohsei, ALON A-6114) was added to maintain the particle dispersion. Here, the appropriate amount of polyelectrolyte was determined by the amount that produced the minimum suspension viscosity. After evacuation in a desiccator to eliminate air bubbles, the

suspension was consolidated by slip casting. The green compacts obtained by the slip casting were further treated by cold isostatic pressing (CIP) at 400MPa for 10min. After drying the compacts at 100°C, sintering was conducted at 1200, 1300 and 1400°C for 2 h in air. The density was measured by Archimedes' method. The phase identification of the sintered specimens was examined by X-ray diffraction (XRD). The microstructures of the sintered specimens were observed by SEM on polished and thermally etched surfaces. The grain growth experiments were conducted in the temperature range of 1450-1600°C with annealing times of 5-75 h for the dense samples of 3YTZ and 3YM-xZT(x=0.95) which had been sintered 1300°C for 2h. The average grain sizes were measured by the linear intercept method⁽¹⁰⁾. Tensile tests were conducted with an Instron-type testing machine for the sample sintered at 1300°C for 2h with gauge dimensions of 7(length)-3(width)-2(thickness) mm in a vacuum.

3. RESULTS AND DISCUSSION

Fig.1 shows the densities of the compacts as-slip casting, further CIP treated and sintered at fixed temperatures. It is seen that the sintering at 1300°C is enough to achieve a full density.

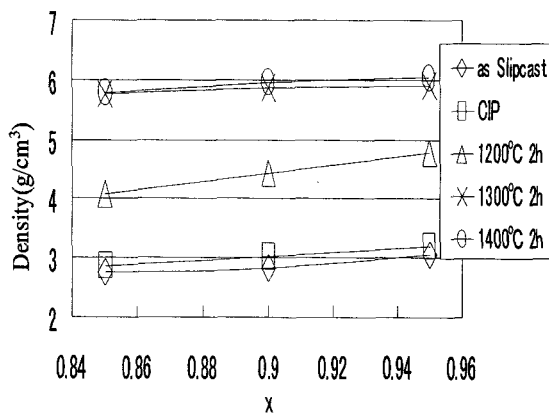


Fig. 1 Density of 3YM-xZT

As an example, Fig.2 shows the XRD pattern of 3YM-xZT(x=0.95) sintered at 1300°C for 2h. It was confirmed that the monoclinic phase did not exist, and the cubic phase only slightly existed.

Fig. 3 shows the average grain sizes sintered at 1300 and 1400°C. The sintered specimens at 1300°C for 2h had the average grain sizes of 0.2 μ m-0.3 μ m depending on the compositions. On the other hand, the sintered specimens at 1400°C for 2h had the average grain sizes of 0.4 μ m-0.7 μ m depending on the compositions. A remarkable grain growth was confirmed. Fig. 4 shows a typical SEM image of the

polished and thermally etched 3YM-xZT(x=0.95) sintered at 1300°C for 2h.

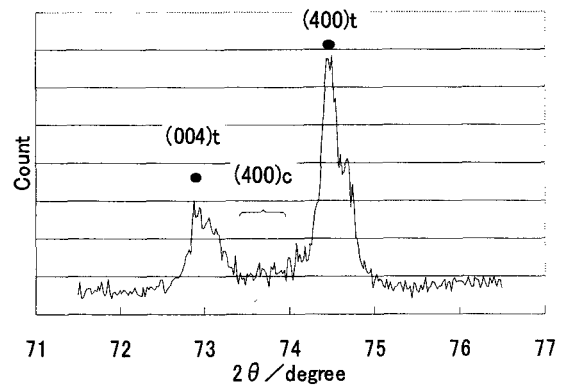
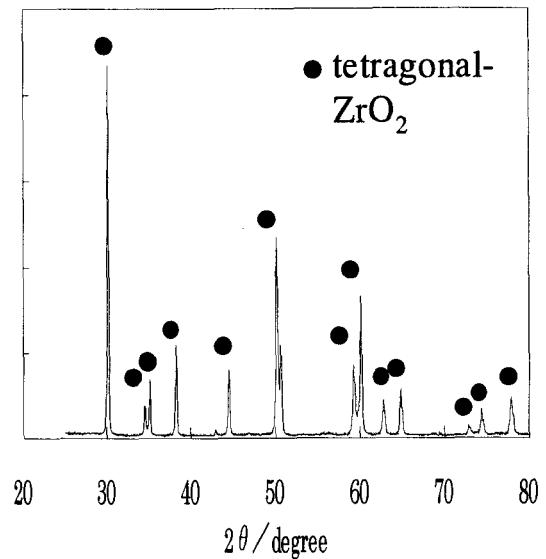


Fig. 2 XRD of 3YM-xZT(x=0.95), after 1300°C for 2h sintering.

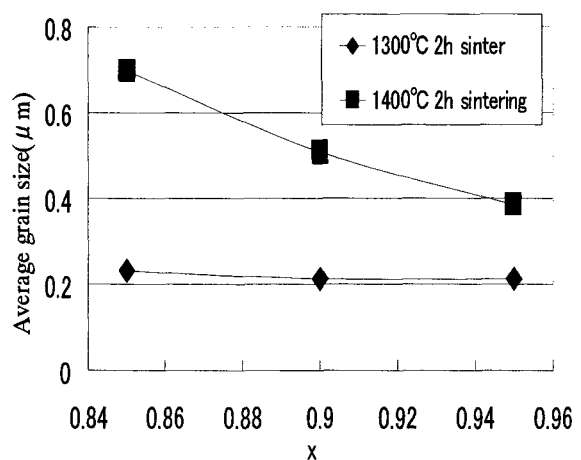


Fig. 3 Average Grain size of 3YM-xZT.

Fine-grain size and dense bodies were obtained, therefore, in this study, sintering condition of 1300°C

for 2h was used for the grain growth experiments and tensile tests.

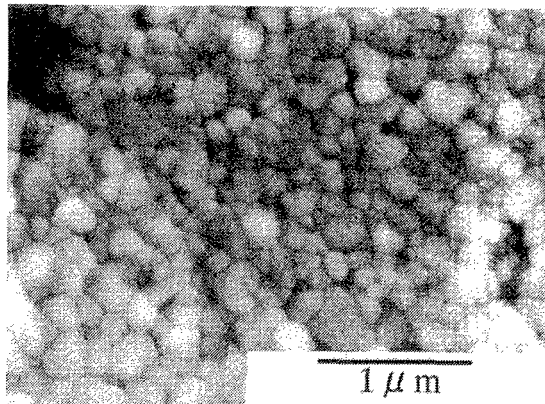


Fig. 4 SEM micrograph of 3YM-xZT(x=0.95), after 1300°C for 2h sintering.

The static grain growths of 3YTZ and 3YM-xZT(x=0.95) were analyzed by the following equation,

$$d_s^r - d_0^r = k \cdot t, \quad (1)$$

where r is the grain growth exponent, d_s is grain size after annealing time t (s), and k is the rate constant. Figs. 5 and 6 show that the static grain growth followed $r=3$, that is, the grain growth is controlled by lattice diffusion.

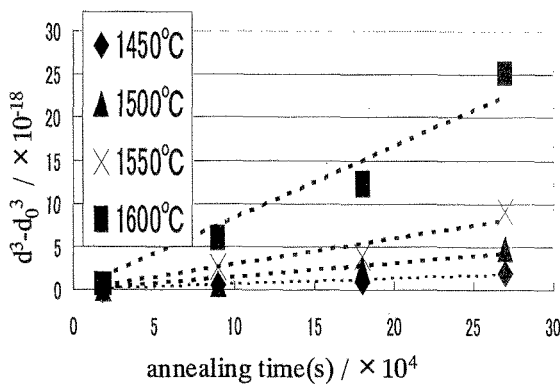


Fig. 5 Grain Growth in 3YTZ at fixed temperatures.

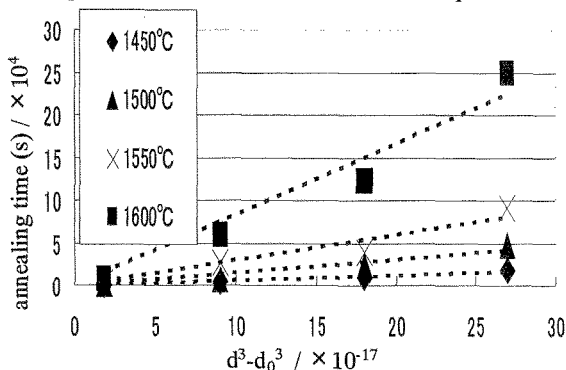


Fig. 6 Grain Growth in 3YM-xZT(x=0.95) at fixed temperatures.

Fig. 7 shows the Arrhenius plots of the grain growth rates. The activation energies of the grain growth rates of 3YTZ and 3YM-xZT(x=0.95) were 554 and 447 kJ/mol, respectively. The activation energy of 3YTZ (554 kJ/mol) corresponds to the previously reported one⁽⁴⁾. The grain growth rate increased and the activation energy decreased by adding TiO₂ and MgO in 3YTZ. Since the cation is much smaller than the oxygen diffusion⁽¹¹⁾, the grain growth was controlled by cation diffusion. Therefore, it is concluded that cation diffusion is enhanced by adding TiO₂ and MgO to ZrO₂.

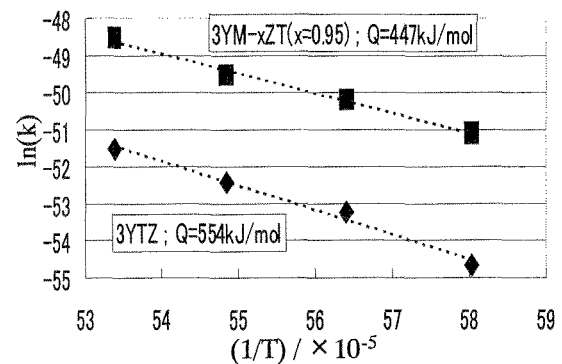


Fig. 7 Arrhenius plots and activation energies in 3YTZ and 3YM-xZT(x=0.95).

Fig. 8 shows that the stress-strain curves of 3YM-xZT(x=0.95) at a constant strain rate of $1.2 \times 10^{-2} \text{ s}^{-1}$. It is seen that the superplasticity at the lower temperature (1350°C) and at the high-strain rate ($1.2 \times 10^{-2} \text{ s}^{-1}$) was realized.

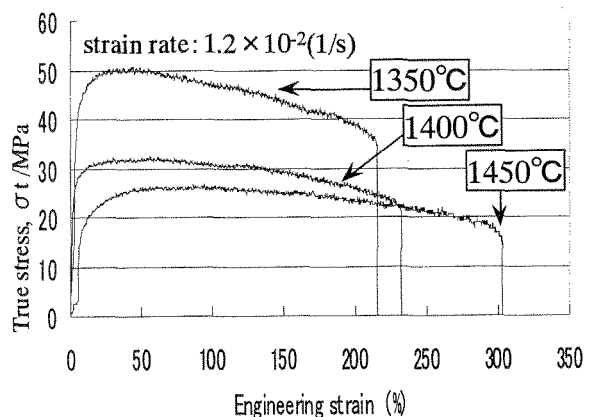


Fig. 8 Stress-strain curves of 3YM-xZT(x=0.95).

To determine the high-deformation rate mechanism, the strain rate ($\dot{\epsilon}$) is analyzed by the following equation,

$$\dot{\epsilon} = A \sigma^n \exp\left(-\frac{Q}{RT}\right); \quad (2)$$

where A is a constant, n is the stress exponent, Q is the

deformation activation energy, R is the gas constant, and T is the absolute temperature. To obtain the n value, tensile tests were conducted at strain rates from 2.4×10^{-3} to $2.4 \times 10^{-2} \text{ s}^{-1}$ and at a constant temperature of 1350°C (Fig.9). The $\ln \dot{\epsilon}$ vs. $\ln \sigma$ plots are shown in Fig.10. Here, the data of 3YTZ that normalized the initial grain size at $0.21 \mu\text{m}$ are also shown⁽¹²⁾.

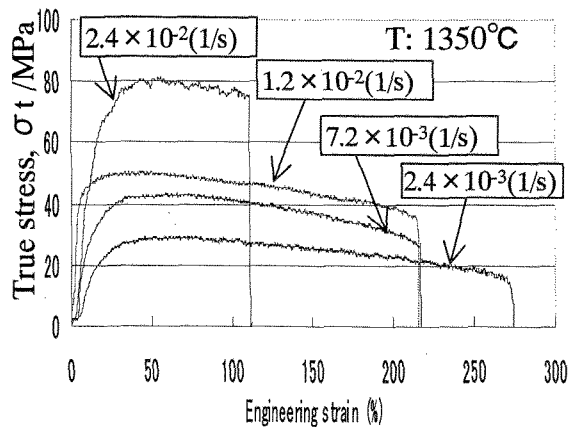


Fig. 9 Stress-strain curves of 3YM-xZT(x=0.95).

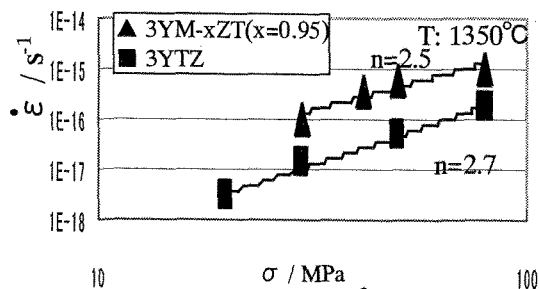


Fig. 10 Relation of $\ln \dot{\epsilon}$ vs. $\ln \sigma$.

It is noted that the plots of 3YM-xZT were expressed as a single line up to the high-deformation rate region, and the n -value is calculated to be 2.5. When the data of 3YTZ is compared with those of 3YM-xZT, it is confirmed that the deformation rate is remarkably enhanced by adding TiO₂ and MgO. This result also indicates that the cation diffusion is enhanced by adding TiO₂ and MgO.

As stated above, the grain growth rate is enhanced by adding TiO₂ and MgO. Therefore, a large grain growth occurred during the tensile test, and the flow stress increased. This seems to be a disadvantage for the superplasticity. Nevertheless, it is confirmed that the tensile ductility of 3YM-xZT ($x=0.95$) is 216 % at the lower temperature of 1350°C and at the high strain rate of $1.2 \times 10^{-2} \text{ s}^{-1}$. By adding TiO₂ and MgO, the grain growth is enhanced and the plastic flow is disturbed. On the other hand, the accommodation process is also enhanced due to the enhancement of

cation diffusion. The relationship between grain growth and the accommodation process are trade offs. In this case, the second one is more effective, and high strain rate superplasticity is achieved for the fine-grained and dense samples.

4. SUMMARY

- 1) The homogeneous microstructure and high density sintered bodies were obtained by colloidal processing.
- 2) The grain growth of 3YTZ and 3YM-xZT ($x=0.95$) was rate-controlled by cation diffusion, and the grain growth rate was enhanced by adding TiO₂ and MgO. The activation energy of the grain growth rate of 3YTZ and 3YM-xZT ($x=0.95$) was 554 and 447 kJ/mol, respectively.
- 3) The high strain rate superplasticity of about 216% was achieved for 3YM-xZT ($x=0.95$) at the strain rate of $1.2 \times 10^{-2} \text{ s}^{-1}$ and at the temperature of 1350°C .

REFERENCES

1. F. Wakai, S. Sakaguchi and Y. Matsuno, *Adv. Ceram. Mater.*, **1** (1986), 259-63.
2. M. Oka, N. Tabuchi and T. Takashi, *Mater. Sci. Forum*, **304-306** (1999), 451-458.
3. K. Morita, K. Hiraga and Y. Sakka, *Key Engineering Materials*, **171-174** (2000), 847-854.
4. K. Sakuma, *Materia Japan*, **37** (1998), 760-766.
5. T. Kondo, Y. Takigawa, T. Sakuma, *Mater. Sci. and Eng.*, **A231** (1997), 163-169.
6. T. Kondo, Y. Takigawa, Y. Ikuhara and T. Sakuma, *Mater. Trans., JIM*, **39** (1998), 1108-1114.
7. S. Prindahl, A. Tholen and T. G. Langdon, *Acta Metall. Mater.*, **43** (1995), 1211-1218.
8. T. S. Suzuki, Y. Sakka and K. Nakano and K. Hiraga, *Mater. Trans., JIM*, **39** (1998), 689-692.
9. Y. Sakka and K. Hiraga, *Nippon Kagaku Kaishi* (1999), 497-506.
10. J. C. Wurst and J. A. Nelson, *J. Am. Ceram. Soc.*, **55** (1972), 109.
11. Y. Sakka, Y. Oishi, K. Ando and S. Morita, *J. Am. Ceram. Soc.*, **74** (1991), 2610-14.
12. K. Morita, unpublished data.

(Received December 7, 2000; Accepted January 31, 2001)